Science Advances

AAAS

advances.sciencemag.org/cgi/content/full/4/5/eaar5251/DC1

Supplementary Materials for

Toward tailoring Majorana bound states in artificially constructed magnetic atom chains on elemental superconductors

Howon Kim, Alexandra Palacio-Morales, Thore Posske, Levente Rózsa, Krisztián Palotás, László Szunyogh, Michael Thorwart, Roland Wiesendanger

Published 11 May 2018, *Sci. Adv.* **4**, eaar5251 (2018)
DOI: 10.1126/sciadv.aar5251

The PDF file includes:

Other Supplementary Material for this manuscript includes the following:
(available at advances.sciencemag.org/cgi/content/full/4/5/eaar5251/DC1)

- movie S1 (.mp4 format). Demonstration of subsequent atom manipulations to construct the close-packed chains of various lengths.
- movie S2 (.mp4 format). Spatially resolved 2D spectroscopic maps for two different ends of the 40-atom-long Fe chain below T_C.
- movie S3 (.mp4 format). Spatially resolved 2D spectroscopic maps for the 40-atom-long Fe chain above T_C.

Supplementary Text

section S1. Ab initio calculations

The system-specific parameters for the tight-binding model calculations displayed in Fig. 4C were obtained in several steps. First, the energetically favored geometries of the Fe atomic structures on the Re(0001) surface have been determined by employing the Vienna Ab-initio Simulation Package (VASP) (*37*). During the calculations the generalized gradient approximation (GGA) in the Perdew–Wang 91 parametrization (PW91) (*38*) of the exchange-correlation functional within density functional theory (DFT) was used. The system was modelled as a 7×7 surface cell in order to avoid interaction of Fe atoms in repetitive supercells, in a slab geometry consisting of four layers of Re (in total $4\times7\times7=196$ Re atoms). The Re atoms in the bottom three layers have been fixed in their hcp bulk positions (in-plane lattice constant of 2.761 Å), and the topmost Re layer and the Fe atomic structures above have been relaxed. A vacuum region of minimum 9 Å thickness has been considered to avoid interaction between repetitive slabs. Due to the large size of the supercell, the Brillouin zone was sampled by the Gamma point only. It was found that the Fe adatom in the hcp hollow site is located closer to the top Re layer (1.84 Å) than the ideal interlayer distance in bulk Re (2.23 Å) due to its small size, and that it displays a stable spin magnetic moment of about $2.86\,\mu_B$. For investigating the geometry of an atomic chain, we considered a 4-atom-long Fe chain, where the Fe atoms reside in neighboring hcp hollow sites. After geometry optimization, we obtained very similar Fe-Re vertical distances of 1.85 and 1.87 Å and spin moments of 2.49 and $2.43\,\mu_B$ for the symmetrically distinct Fe atoms in the chain (outer and inner, respectively) as for the adatom case. Due to this similarity, we determined the tight-binding model parameters from calculations performed for the adatom case.

section S2. Model parameters

The on-site energy for the *d* electrons μ, the spin-splitting parameter J and the spin–orbit coupling strength λ used in the tight-binding model calculations were derived by investigating the resonance energies ε_n of the single-site potentials obtained self-consistently from SKKR and the Embedded Cluster methods (*39*). These resonance energies are associated with the eigenvalues of the effective one-electron Hamiltonian

$$H=\mu\boldsymbol{c}^{\dagger}\boldsymbol{c}+\boldsymbol{c}^{\dagger}(L_0\otimes JS^{Z})\boldsymbol{c}+\lambda\boldsymbol{c}^{\dagger}(\boldsymbol{LS})\boldsymbol{c} \qquad (1)$$

where $\boldsymbol{c}$ denotes the electron annihilation operators in the *d* states, $\boldsymbol{S}$ is the operator of the one-half spin of electrons, $\boldsymbol{L}$ stands for the angular momentum operator restricted to the *d* $(l=2)$ states, L_0 denotes the unit matrix in the same subspace, and $\boldsymbol{LS}=L^x\otimes S^x+L^y\otimes S^y+L^z\otimes S^z$. Note that in the Hamiltonian given by Eq. (1) we supposed that the exchange field is oriented along the *z* axis; however, this choice does not influence the eigenvalues. The on-site energy μ is given on a scale where the Fermi energy of the Re substrate corresponds to zero.

The parameters for the tight-binding model were determined from the self-consistent calculations performed for the Fe adatom. The resonance energies of the Fe potential showed basically a double-split, the two branches displaying five lines with almost equidistant separation. This situation typically corresponds to the case of large spin splitting (J) and small spin–orbit coupling (λ) as also discussed in ref. (*39*). Expanding perturbatively up to first order in λ, the eigenvalues

of H can be written as $\varepsilon_{m_l}^{\pm} = \mu \pm \frac{J}{2} \pm \frac{\lambda}{2} m_l$, $\pm$ denoting to the up- and down-spins and m_l =–2, –1, 0, 1, 2. This procedure led to the parameter values μ =–0.92 eV, J =2.18 eV and λ =0.06 eV.

section S3. Tight-binding model

In order to deduce the topological character of the electronic phase, we implemented a Slater–Koster tight-binding model (*40*, *41*) for the linear Fe chain. Our model is material-specific, based on the experimentally determined superconducting gap, the parameter values determined from *ab initio* calculations discussed above and hopping parameters from ref. (*42*). The Hamiltonian of the system reads

$$H = \sum_{\boldsymbol{r}} \mu \boldsymbol{c}_{\boldsymbol{r}}^{\dagger} \boldsymbol{c}_{\boldsymbol{r}} + \sum_{\boldsymbol{r},\delta\boldsymbol{r}} \boldsymbol{c}_{\boldsymbol{r}+\delta\boldsymbol{r}}^{\dagger} T(\delta\boldsymbol{r}) \boldsymbol{c}_{\boldsymbol{r}} + \lambda \sum_{\boldsymbol{r}} \boldsymbol{c}_{\boldsymbol{r}}^{\dagger} (\boldsymbol{L}\boldsymbol{S}) \boldsymbol{c}_{\boldsymbol{r}} + \sum_{\boldsymbol{r}} \boldsymbol{c}_{\boldsymbol{r}}^{\dagger} (L_0 \otimes J\boldsymbol{m}(\boldsymbol{r})\boldsymbol{S}) \boldsymbol{c}_{\boldsymbol{r}} + \left(\sum_{\boldsymbol{r}} \Delta \boldsymbol{c}_{\boldsymbol{r}}^{\dagger} (L_0 \otimes i\sigma^y) \boldsymbol{c}_{\boldsymbol{r}}^{\dagger} + h.c. \right) \quad (2)$$

Similarly to Eq. (1), $\boldsymbol{c}_{\boldsymbol{r}}$ are vectors containing the annihilation operators of the electrons in the *d* orbitals. The sums in $\boldsymbol{r}$ and $\delta\boldsymbol{r}$ run over the positions of the Fe atoms in the chain and the nearest-neighbor vectors, respectively. The coefficients μ, T, λ, J and Δ describe on-site energies, hopping matrices, spin–orbit coupling, spin splitting and superconducting pairing potential, respectively. The spin $\boldsymbol{S} = \frac{1}{2}(\sigma^x, \sigma^y, \sigma^z)$ is expressed by the Pauli matrices, the standard two-dimensional generators of *SU(2)*. The orbital moment $\boldsymbol{L}$ is given on the five-dimensional basis of the orbitals by the following representation of *SO(3)*

$$L_1 = i \begin{pmatrix} 0 & 0 & 1 & 0 & 0 \\ 0 & 0 & 0 & 1 & \sqrt{3} \\ -1 & 0 & 0 & 0 & 0 \\ 0 & -1 & 0 & 0 & 0 \\ 0 & -\sqrt{3} & 0 & 0 & 0 \end{pmatrix} \quad (3)$$

$$L_2 = i \begin{pmatrix} 0 & 1 & 0 & 0 & 0 \\ -1 & 0 & 0 & 0 & 0 \\ 0 & 0 & 0 & -1 & \sqrt{3} \\ 0 & 0 & 1 & 0 & 0 \\ 0 & 0 & -\sqrt{3} & 0 & 0 \end{pmatrix} \quad (4)$$

$$L_3 = i\begin{pmatrix} 0 & 0 & 0 & -2 & 0 \\ 0 & 0 & -1 & 0 & 0 \\ 0 & 1 & 0 & 0 & 0 \\ 2 & 0 & 0 & 0 & 0 \\ 0 & 0 & 0 & 0 & 0 \end{pmatrix} \quad (5)$$

These operators are expressed in the real basis xy, yz, zx, $x^2 - y^2$, $3z^2 - r^2$ of the orbital angular momentum.

The non-collinear magnetization of the chain is encoded in $\boldsymbol{m}(\boldsymbol{r})$. Since the experimental data suggest a modulation of both the in-plane and out-of-plane magnetization components with a period of $4\,a_{\mathrm{Re}}$ (see fig. S2), we considered a spin spiral rotating in the plane defined by the Fe chain and the out-of-plane direction with an angle of 90° between adjacent atoms. The choice of the rotational plane is also supported by symmetry considerations, which prefer this type of so-called cycloidal spin spiral states in surface magnetic structures due to the presence of the Dzyaloshinsky–Moriya interaction (*29*). As demonstrated in ref. (*43*), the non-collinear magnetic structure is equivalent to a ferromagnetic chain with an additional Rashba term, and this latter model was investigated in earlier publications (*41*).

The hopping matrices T between neighboring atoms mix the *d* orbitals (*40*), being of the form

$$T(\delta\boldsymbol{r}) = \sum_\alpha V^{dd\alpha}(|\delta\boldsymbol{r}|)E^{dd\alpha}(\delta\boldsymbol{r}/|\delta\boldsymbol{r}|) \otimes \sigma_0 \quad (6)$$

where α runs over σ, π and δ orbitals. Here, $V^{dd\alpha}$ are Slater–Koster two-center parameters in orthogonal basis and $E^{dd\alpha}$ are Slater–Koster matrices (*40*, *42*). The parameter-specific integrals $V^{dd\alpha}$ are derived from the Fe bulk values given in ref. (*42*) by scaling in order to account for the different lattice spacing that the Fe atoms assume on the Re surface. The expression for the scaling reads $V^{dd\alpha} = (a_{\mathrm{Re}}/a_{\mathrm{Fe}})^{-n^\alpha} V^{dd\alpha}_{\mathrm{Fe\,bulk}}$, with a_{Re} =2.761 Å the in-plane lattice constant of the hcp Re substrate, a_{Fe} =2.477 Å the distance between nearest neighbors in bulk bcc Fe, and the exponents $n^\sigma = 3$ and $n^\pi = n^\delta = 4$ (see ref. (*41*)). The rescaled parameters used for the calculations are $V^{dd\sigma} = -0.48$ eV, $V^{dd\pi} = 0.26$ eV and $V^{dd\delta} = -0.02$ eV. The effect of the Re surface is included in the proximity-induced superconductivity term $\Delta = 0.28$ meV, which was determined experimentally.

The Hamiltonian given by Eq. (2) is not time-reversal symmetric and it is classified by a $\mathbb{Z}_2$ topological invariant (*44*), being in the symmetry class with Cartan label *D* according to the classification in ref. (*45*). This invariant, called Majorana number, is given by (*46*)

$$\mathcal{M} = \mathrm{sgn}\left(Pf\left(\tilde{\mathrm{B}}(0)\right)Pf\left(\tilde{\mathrm{B}}(\pi)\right)\right) \tag{7}$$

where Pf denotes the Pfaffian of an antisymmetric matrix and $\tilde{\mathrm{B}}$ is the Fourier transform of the matrix B defined such that

$$\mathcal{H} = \sum_{\mathbf{r}_1,\mathbf{r}_2} \boldsymbol{\gamma}_{\mathbf{r}_2}^T B(\mathbf{r}_2 - \mathbf{r}_1)\boldsymbol{\gamma}_{\mathbf{r}_1} \tag{8}$$

with $\boldsymbol{\gamma}_{\mathbf{r}} = (\gamma_{\mathbf{r},i,l,s})_{i\in(1,2),l\in(-2,-1,0,1,2),s\in(\uparrow,\downarrow)}$ being a vector containing the Majorana operators

$$\begin{aligned}\gamma_{\mathbf{r},1,l,s} &= c^{\dagger}_{\mathbf{r},l,s} + c_{\mathbf{r},l,s} \\ \gamma_{\mathbf{r},2,l,s} &= i(c^{\dagger}_{\mathbf{r},l,s} - c_{\mathbf{r},l,s})\end{aligned} \tag{9}$$

with the l and s indices describing the angular momentum and spin quantum numbers. The Majorana number in Eq. (7) takes the value of $\mathcal{M} = 1$ in the topologically trivial and $\mathcal{M} = -1$ in the topologically non-trivial phase, shown in Fig. 4C.

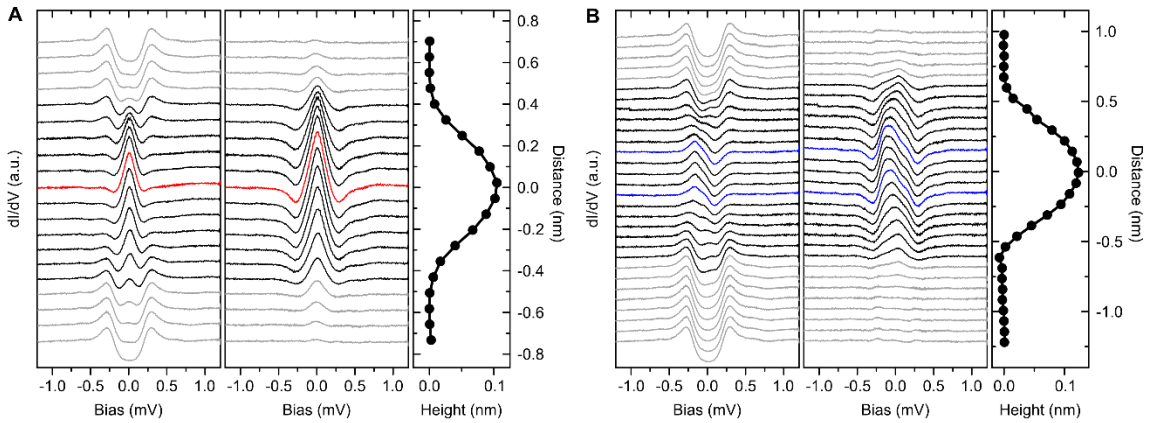

fig. S1. Spatial distribution of the YSR states for a single Fe atom and an Fe dimer on the Re(0001) surface. (**A** and **B**) Spatially-resolved dI/dV spectra across (A) a single Fe atom and (B) an Fe dimer. The raw spectra are presented at the left, the spectra after subtracting the spectrum on the bare Re substrate in the middle, and the corresponding surface profile on the right. The dots indicate the locations where the spectra were obtained. The spectra obtained within atomic protrusions in the topographic profiles are plotted in black for both panels, while grey denotes spectra obtained above the Re substrate. The spectra taken just above the Fe atoms are depicted in red for the single Fe atom and in blue for the Fe dimer in panels (A) and (B), respectively. For both the single atom and the dimer, the intensity of the YSR peak decays within a few atomic lattice constants (~1 nm) inside the Re substrate, with spatial variations of the spectral shape.

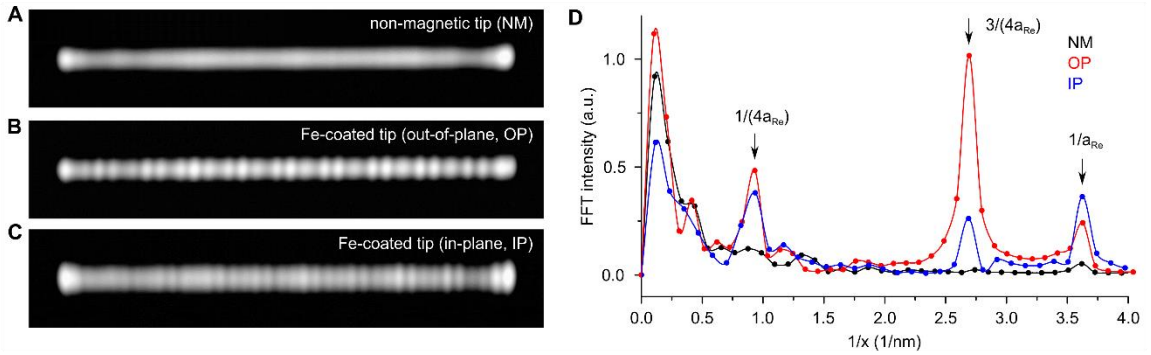

fig. S2. The fast Fourier transformation analysis for the magnetic structure of the 40-atom-long Fe chain. (**A**)-(**C**) Contrast-adjusted (SP)-STM images measured with (A) a non-magnetic PtIr tip and Fe-coated tips sensitive to (B) the out-of-plane and (C) the in-plane component of the magnetization along the chain. The (SP)-STM data are identical to the ones displayed in Figs. 2C-E. (**D**) FFT analysis plot for determining the period of the modulations observed in the (SP)-STM profiles with the three different tips. There are two dominant periodic modulations, $4\,a_{\mathrm{Re}}$ ~1.1 nm and $4/3\,a_{\mathrm{Re}}$ ~0.36 nm, which are visible in the FFT spectra obtained with both spin-sensitive Fe coated tips, but are absent for the one taken with the non-magnetic tip. The contribution of the atomic corrugation in the Fe chain appears at $1/a_{\mathrm{Re}}$ in all three FFT spectra.

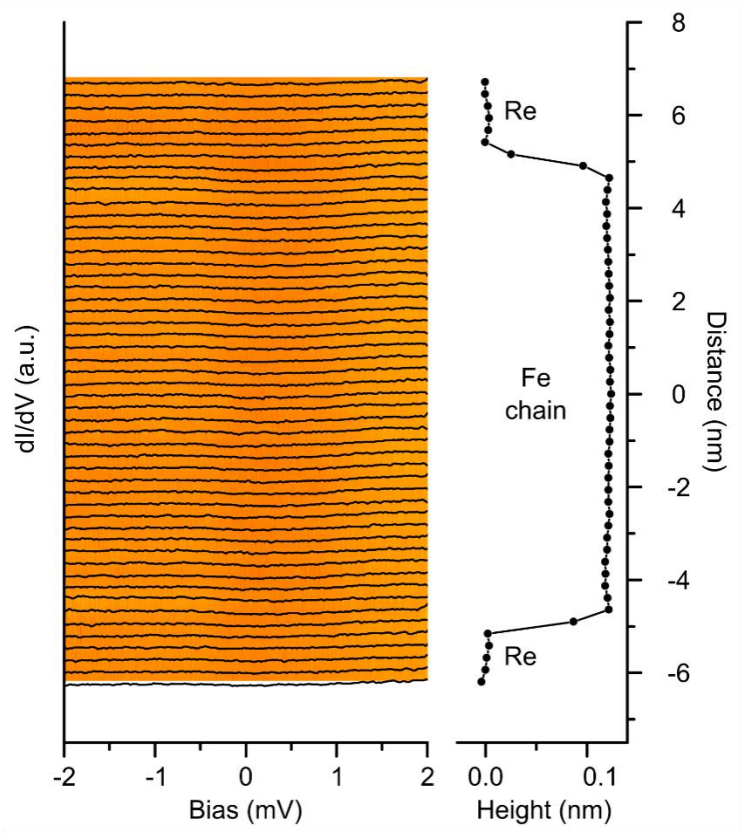

fig. S3. Absence of the in-gap states on the 40-atom-long Fe chain above the superconducting critical temperature of Re. (left) Spatially-resolved dI/dV spectra and colour-coded spectroscopic map along the chain taken at a temperature above the superconducting critical temperature of the Re (T=1.7 K, tunneling parameters I_T=5.0 nA, V_S=3.0 mV). The spectra taken on both the Re substrate and the Fe chain display a featureless almost constant LDOS at the Fermi energy. This indicates that superconductivity of the Re substrate is fully suppressed and all in-gap features on the Fe chain have disappeared. (right) Simultaneously obtained topographic profile during the spectroscopic measurement. The dots indicate the spatial positions where the spectra were obtained.

movie S1. Demonstration of subsequent atom manipulations to construct the close-packed chains of various lengths.

movie S2. Spatially resolved 2D spectroscopic maps for two different ends of the 40-atom-long Fe chain below T_C.

movie S3. Spatially resolved 2D spectroscopic maps for the 40-atom-long Fe chain above T_C.